New Lower Bound Techniques for Robot Motion Planning Problems

John Canny

Artificial Intelligence Laboratory, Massachusetts Institute of Technology
and
Computer Science Division, University of California, Berkeley

John Reif

Computer Science Department, Duke University

Abstract We present new techniques for establishing lower bounds in robot motion planning problems. Our scheme is based on *path encoding* and uses homotopy equivalence classes of paths to encode state. We first apply the method to the shortest path problem in 3 dimensions. The problem is to find the shortest path under an L^p metric (e.g. a euclidean metric) between two points amid polyhedral obstacles. Although this problem has been extensively studied, there were no previously known lower bounds. We show that there may be exponentially many shortest path classes in single-source multiple-destination problems, and that the single-source single-destination problem is NP-hard. We use a similar proof technique to show that two dimensional dynamic motion planning with bounded velocity is NP-hard. Finally we extend the technique to compliant motion planning with uncertainty in control. Specifically, we consider a point in 3 dimensions which is commanded to move in a straight line, but whose actual motion may differ from the commanded motion, possibly involving sliding against obstacles. Given that the point initially lies in some start region, the problem of finding a sequence of commanded velocities which is guaranteed to move the point to the goal is shown to be non-deterministic exponential time hard, making it the first *provably* intractable problem in robotics.

1 Introduction

The object of robot motion planning is to find a sequence of motions which is guaranteed to move the robot to its goal, while avoiding obstacles in the robot's environment. There may also be a cost function on the trajectory which is to be minimized. In this paper we give new lower bounds for three fundamental classes of motion planning problems: shortest path, dynamic motion planning, and motion planning in the presence of uncertainty.

Acknowledgements. This reseach was sponsored in part by the NSF under contract NSF-DCR-85-03251 and the Office of Naval Research under Office of Naval Research contracts N00014-81-K-0494 and N00014-80-C-0647 and in part by the Advanced Research Projects Agency under Office of Naval Research contracts N00014-80-C-0505 and N00014-82-K-0334. John Canny was supported by an IBM fellowship.

The authors would also like to thank Prof. John Hopcroft, Prof. Michael Brady and Dr. Joseph Mundy for organising, and the NSF (under contract DCR-8605077) for sponsoring the geometric reasoning workshop at Keble College in June-July 1986, at which the preliminary work for this paper was performed.

The simplest motion planning problem is the find-path or generalized movers' problem, in which the objective is to find any collision-free path. This problem reduces to a point navigation problem in the configuration space of the robot, [LW]. It is solvable in polynomial time if the number of degrees of freedom is fixed, [SS] and [KY], by adding adjacency information to cell-decomposition algorithms of [Col] and [BKR]. A new method based on singularity theory was recently described [Ca], which runs in time polynomial in the environment size for a fixed number of degrees of freedom, with an exponent equal to the number of degrees of freedom, which is worst-case optimal. Here we show that three natural extensions to the find-path problem are difficult even in three dimensions.

1.1 Lower Bound Techniques for Robot Motion Planning

The first hardness results for robot motion planning were due to Reif [Re] who showed that the generalized movers' problem is PSPACE-hard. Other authors have produced PSPACE hardness results with many movable objects in the plane [HSS]. In these proofs the number of degrees of freedom grows with the problem size. Of a different character were the results of Reif and Sharir [RSh] on dynamic motion planning, where PSPACE and NP-hardness results were established for motion planning with a fixed number of degrees of freedom among obstacles moving in a known way. Natarajan [Na] recently gave a PSPACE-hardness proof for motion planning with uncertainty under a certain dynamic model, [LMT].

In all the results that follow, the environment consists of polyhedral obstacles, and the coordinates of points, equations of face normals etc. are assumed to be expressed as rational quotients of binary integers. The size of the description is the sum of number of features and the lengths of all binary numbers in the description.

In this paper we present three proofs using a new technique called *path encoding*. Our results apply to problems in which the number of degrees of freedom is small and fixed. In path encoding we represent discrete state using homotopy equivalence classes of paths. In both proofs, we generate exponentially many path classes in a fixed 3-dimensional polyhedral environment. In the first two proofs of NP-hardness of shortest path and dynamic motion planning, each path class represents a satisfying assignment to a set of boolean variables.

0272-5428/87/0000/0049$01.00 © 1987 IEEE

In the third proof, non-deterministic exponential time hardness of compliant motion planning with uncertainty, we use path classes to represent the contents of a exponential-length Turing machine tape.

1.2 The Shortest Path Problem

The shortest path problem is of interest in robotics because it is the simplest instance of a minimum cost path planning problem. The *L^p-shortest path problem*, may be defined in two or three dimensions as the problem of finding the shortest obstacle-avoiding path between two given points under an L^p metric, with polygonal or polyhedral obstacles respectively. Efficient algorithms for two dimensional euclidean shortest path have been known for some time. This problem was first studied by Lozano-Pérez and Wesley [LW]. No upper bounds were given in their paper, but their algorithm should run in $O(n^3)$ time. Improvements were given by Sharir and Schorr [SSc], and by Reif and Storer [RS] $O(n(k+\log n))$ time, where k is the number of convex parts of the obstacles. Mitchell and Papadimitriou gave a polynomial time algorithm for a generalization of the problem analagous to finding the shortest path for a light ray through polygonal regions of different refractive index [MP].

While the euclidean shortest path has efficient solutions in two dimensions, the three-dimensional problem is much more difficult. There have been a number of papers on restricted versions of the problem. Mount [Mo], and Sharir and Baltsam [SB] gave polynomial time algorithms for environments consisting of a small fixed number of convex polyhedra. Papadimitriou [Pa] gave a polynomial time approximate algorithm which finds a path at most a small multiplicative constant longer than the shortest path. The general problem has been dealt with by Sharir and Schorr [SSc] who gave an $2^{2^{O(n)}}$ algorithm by reducing the problem to an algebraic decision problem in the theory of real closed fields. The best bound is due to Reif and Storer [RSt] who gave both $2^{n^{O(1)}}$-time, and $(n^{O(\log n)})$-space algorithms by using the same theory but with a more efficient reduction. To date, in spite of the absence of efficient algorithms for the general problem, no lower bounds were known.

1.3 Dynamic Motion Planning with Velocity Bounds

We consider motion planning for a robot with a fixed number of degrees of freedom in an environment in which the obstacles are moving, and in which the robot has constraints on its velocity. If there are no motion constraints, and the trajectories of obstacles can be described algebraically, then the problem is solvable in polynomial time [RSh]. However, if velocity limits are added, the problem is more difficult. In [RSh] it was shown that motion planning in 3-d with rotating dynamic obstacles is PSPACE-hard in the presence of velocity bounds, and NP-hard in the absence of bounds. However, the rotating obstacles have non-algebraic trajectories. Here we give the much stronger result that motion planning for a point in the plane with velocity bounds is NP-hard, even when the moving obstacles are convex polygons moving with constant linear velocity without rotation.

We define the *2-d asteroid avoidance problem* as the problem of determining a collision-free path for a point in the plane with bounded velocity magnitude, with convex polygonal obstacles moving with fixed linear velocity (no rotation). The obstacles are assumed not to collide.

1.4 Compliant Motion Planning with Uncertainty

We also treat motion planning with uncertainty, where the objective is to produce a plan which is guaranteed to succeed even if the robot cannot perfectly execute it due to control error. With control uncertainty, it is impossible to perform assembly tasks which involve sliding motions using only position control. Robot control uncertainty is significant and has traditionally biased robot applications toward low-precision tasks such as welding and spray-painting. To successfully plan high-precision tasks such as assembly operations, uncertainty must be taken into account, and other types of control must be used which allow *compliant motion*. Compliant motion ([In], [Ma]) occurs when a robot is commanded to move into an obstacle, but rather than stubbornly obeying its motion command, it complies to the geometry of the obstacle.

Compliant motion is possible only with certain dynamic models. The two most common of these are the generalized spring and generalized damper models, [Ma]. Our proof will succeed with either of these models, but the one we will use is a simplified version of the damper model described in [LMT]. We assume that our environment describes the configuration space of the robot, so that the robot itself is always a point. The planned path consists of straight-line commanded motions each for a fixed time interval. That is, at the i^{th} step, the point is commanded to move at velocity v_i for time t_i. Because of control uncertainty however, the

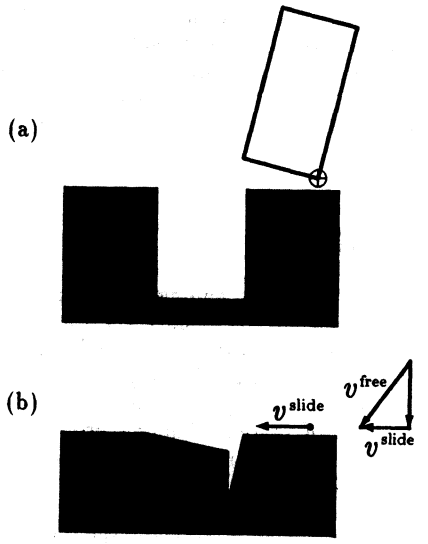

Figure 1: (a) Peg and hole environment, (b) Configuration space showing locus of reference point of peg during compliant motion.

point actually moves with a velocity v_i^{free} which lies in a ball of radius ϵv_i about the commanded velocity, i.e.

$$||v_i^{free} - v_i|| < \epsilon v_i \tag{1}$$

Without loss of generality, we assume all v_i have unit magnitude, and scale the t_i accordingly.

For a compliant motion, the object moves along an obsta-

cle surface with a sliding velocity v_i^{slide} which is the projection onto the surface of some v_i^{free} satisfying (1). This v_i^{free} must point into the surface, as shown in figure 1. Figure 1a shows a side view of a peg-in-hole insertion, while 1b shows the obstacle in configuration space seen by the reference point on the peg. The motion of the peg (without rotation) can be determined from the motion of the reference point based on generalized damper dynamics. We will not consider further details of the dynamic model since they are not necessary for our proof, but we recommend the reference [LMT].

The *Compliant Motion Planning with Uncertainty* problem is to find a sequence of motions v_i, which is guaranteed to move every point in a polyhedral start region S into a polyhedral goal region G, moving among and possibly sliding on polyhedral obstacles. Each motion is subject to a velocity uncertainty ϵ as described above. We consider a polyhedral start region because there will inevitably be some uncertainty in the initial position of the point. That is, we know that p is initially somewhere in S but we cannot know where exactly. However, because our plan succesfully moves every point in S into G, it is guaranteed to move p from its actual position into G. In [Na] it is shown that this problem is PSPACE-hard. Using some of the new techniques in this paper, we are able to show that 3-d compliant motion planning is non-deterministic exponential time hard. We believe this to be the first instance of a *provably* intractable problem in robotics.

1.5 Outline of Paper

In section 2 we give a brief description of the path encoding technique for NP-hardness proofs, and describe the main structures required. We then complete this section with lower bounds on the number of shortest path classes in a polyhedral environment, and a proof of NP-hardness for the shortest path problem.

Section 3 gives a similar proof of NP-hardness for 2 dimensional dynamic motion planning with velocity limits (the "asteroid avoidance" problem).

Section 4 begins with a description of a simplified dynamic model for compliant motion planning with uncertainty. Then we describe a class of polyhedral environments for which finding a guaranteed motion plan is non-deterministic exponential-time hard.

2 Lower Bounds for the Shortest Path Problem

2.1 Path Encoding for Shortest Paths

First we define the *shortest route* from any point x in space to a source q as the sequence of environment edges traversed by the shortest path from x to q. In some cases there may be more than one shortest route from x to q. Then we define an equivalence relation such that two points are equivalent iff they have the same set of shortest routes to q. This equivalence relation gives us a partition of free space and allows us to speak of *shortest path classes.*

To simplify things we will only examine these classes at certain "one dimensional" slits. These slits actually have some finite width ϵ and lie in horizontal plates of thickness also ϵ. In our construction it is possible to represent the path classes within a slit using the concept of a "virtual source".

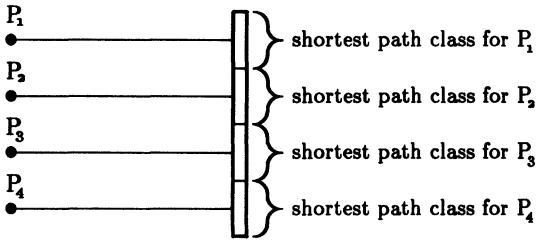

Figure 2: Path Classes and virtual sources for a single slit.

A virtual source is a point p_i such that the actual distance from a point x in the path class to the start point is the same (to within a small additive error) as the straight line distance from x to p_i. The straight line is often referred to as an "unfolding" of the actual path. Each shortest path class has its own virtual source, and the sources will be evenly spaced and equidistant from the slit as shown in figure 2.

2.2 The Environment

We will be generating (2^n) path classes in our construction, and each class may be thought of as encoding an n-bit binary string, $b_1, \ldots b_n$. The construction may be broken down into three types of substructure:

- Path Splitter: This doubles the number of shortest path classes by splitting them.
- Path Shuffler: Performs a perfect shuffle of path classes.
- Literal Filter: Filters for those paths which have a particular bit equal to zero or one in their encoding.

Path Splitter

The path splitter has the property that if its input slit contains n shortest path classes as described above, its output slit will contain $2n$ path classes. A splitter consists of a stack of 3 horizontal plates separated by ϵ, and is shown from above in figure 3. The top plate covers the x-y plane except for the input slit S_{in}. The middle plate has two slits at 45°, labelled S_1 and S_2, and the bottom plate contains the output slit S_{out}. Any shortest path from S_{in} to S_{out} passes through either S_1 or S_2.

The splitter uses the unfolding of paths to generate many virtual sources. The principle of path unfolding is illustrated in figure 3. For any point p in the output slit S_{out}, the shortest path from that point to the virtual source P_1 consists of two straight line segments which make equal angles with S_2 (actually this is only true in the limit as $\epsilon \to 0$, but we will deal with the finite ϵ case shortly). By mirror symmetry there is a second virtual source P_1' such that the distance of the shortest path from it any point p in S_{out} to P_1 is the same as the *straight line distance* from p to P_1'.

Suppose we have n virtual sources for the n shortest path classes in S_{in}. We have seen that S_2 behaves like a mirror and reflects each virtual source P_i to a new position P_i'. Since S_1 also produces a reflected copies P_i'' of the P_i, S_{out} now sees $2n$ virtual sources, as shown in figure 4. In other words there are twice as many shortest path classes in S_{out} because each path class from S_{in} bifurcates into a class that passes through

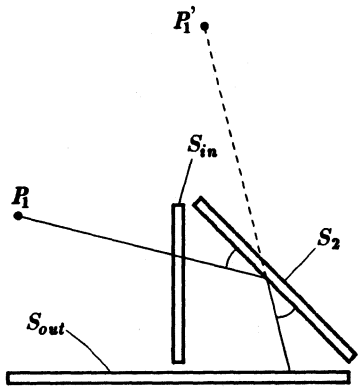

Figure 3: Path splitter, showing the principle of path unfolding.

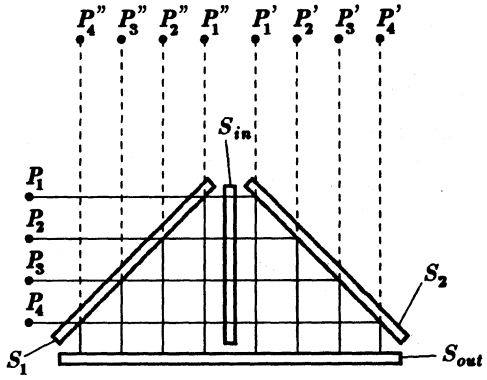

Figure 4: Path splitter showing doubling of the number of path classes.

S_1 and a class that passes through S_2. The distance between path classes remains the same, so the output slit of a splitter is twice the length of its input slit.

The geometric argument above is only true if the plates have zero thickness and slits have zero width, however it does give valid lower bounds for a finite thickness, finite width environment. In section 2.4, we derive upper bounds which differ by an additive multiple of ϵ. With these bounds and a sufficiently small ϵ, we can guarantee that path classes remain distinct, and in section 2.5, we show that the three-dimensional environment has a polynomial size description.

Path Shuffler

A shuffler is shown from above in figure 5. It consists of 4 horizontal plates of width and spacing ϵ. The top two plates simply separate the top and bottom halves of the input slit, as shown in figure 5(a). The second, third and fourth plates behave rather like a twisted splitter. The second plate contains the two slits S_1 and S_2, the third plate contains the diagonal slits S_3 and S_4, and the fourth plate contains the output slit S_{out}. Paths from S_1 to S_{out} are constrained by a barrier to pass through S_3. Thus S_3 acts as a mirror and produces a copies of the virtual sources in S_1. S_4 produces a similar copies of the sources in S_2, however these two images are displaced by half the source spacing δt. This has the effect of interleaving the two sets of path classes, so the class

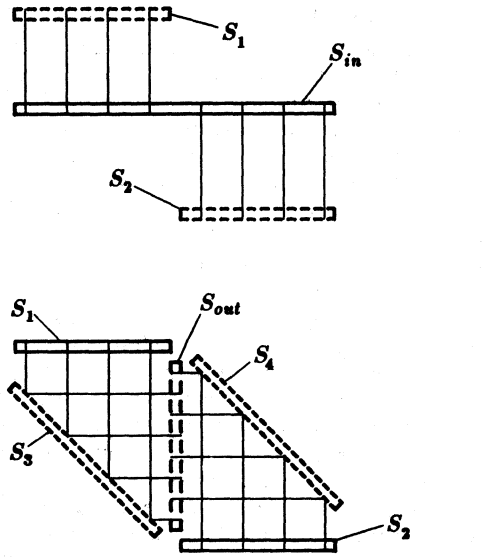

Figure 5: Path shuffler. The first two plates are shown at the top, and plates two, three, and four at the bottom of the figure.

numbers of the lower half ($b_1 = 0$) of the input slit are doubled, while the path numbers of the upper half ($b_1 = 1$) are doubled and incremented. This corresponds to a left shift of the encoding with wrap around of the leading bit, i.e. a circular left-shift. The spacing between path classes is halved, so the output slit of a shuffler has half the length of its input slit.

Literal Filter

The literal filter is designed to filter for those path classes whose encodings have a zero or a one in the i^{th} bit. We do this by stretching all other path classes. Recall that the j^{th} path class encodes a binary string $b_1, \ldots b_n$. To filter for paths having $b_i = 0$, we put a barrier in the way of paths having $b_i = 1$. The problem with doing this on the original encoding is that the barrier may need to be split into exponentially many sections, e.g. for b_n we need to cover every second path class. Instead we use shufflers to rotate the encoding so that the i^{th} bit becomes the most significant bit of the encoding, at which point all paths having $b_i = 1$ are in the same half of the slit.

A literal filter for $b_i = 0$ is shown in figure 6. A single shuffler performs a 1-bit left shift of the encoding, and after cascading $(i-1)$ shufflers, the encoding becomes $b_i, \ldots b_n, b_1, \ldots b_{i-1}$. Once the i^{th} bit has become the most significant bit, we block off the upper half of the slit. We then add $(n - i + 1)$ more shufflers to restore the original encoding. Now the paths which have $b_i = 1$ will have been stretched slightly by having to travel around the barrier. In section 2.4, equation (11) we give bounds on the amount of stretching necessary, and show that stretched paths can be distinguished from unstretched ones.

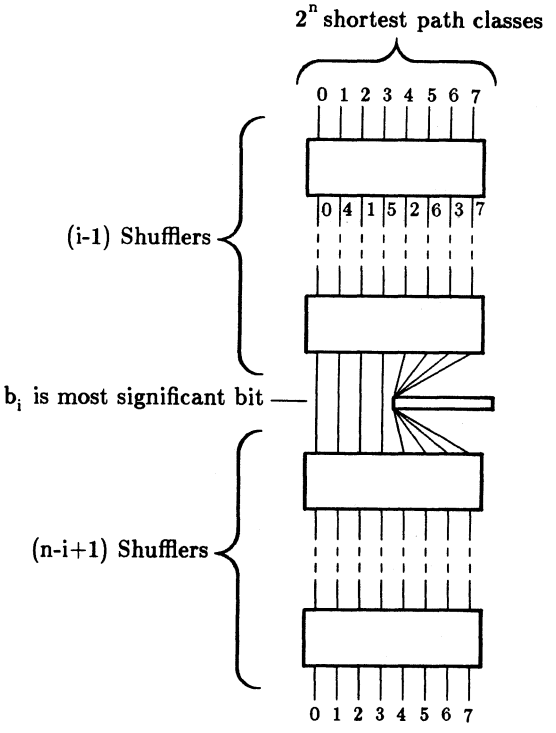

Figure 6: A literal filter with barrier to stretch paths having $b_i = 1$.

2.3 Lower Bounds for 3-d Shortest Path

The following theorem follows immediately from the properties of splitters:

Theorem 2.3.1 *The number of shortest path classes in a polyhedral environment may be exponential in the number of faces, edges and vertices in the environment, and* $\Omega(2^{\sqrt{N}})$ *where* N *is the length of the description of the environment.*

Proof We cascade n splitters each of which has constant number of faces, edges and vertices, giving us 2^n shortest path classes. Applying the results of section 2.5, we need only $O(n)$ bits to describe each environment vertex (since there are no shufflers), and thus $N = O(n^2)$ bits for the whole environment. □

Theorem 2.3.2 *The problem of finding a shortest path under any* L^p *metric in a three-dimensional polyhedral environment is NP-hard.*

Proof Given a 3-SAT formula, we construct a polyhedral environment, and source and target points, such that knowledge of the shortest path between source and target allows us to decide in polynomial time if the formula is satisfiable. The size of the environment description is polynomial in the formula size.

Recall that a 3-SAT formula in n variables $b_1, \ldots b_n$ has the form

$$\bigwedge_{i=1,\ldots m} C_i \qquad (2)$$

where each C_i is a clause of the form $(l_{i1} \vee l_{i2} \vee l_{i3})$. Each literal l_{ij} in turn, is either a variable or the negation of a variable. The size of the formula can be measured as the sum of the number of variables n and the number of clauses m.

First we cascade n splitters below the source point, to give us 2^n shortest path classes. Each path encodes an assignment to the n variables through the binary representation of the path number. Then we progressively filter out those classes whose encodings do not satisfy a particular clause in the formula.

To filter for a particular clause, we place 3 literal filters in parallel (each consisting of n shufflers) as shown in figure 7. This structure implements a disjunction of literals because if an assignment satisfies any of the three literals there will be a short path through the corresponding literal filter. The collection of literal filters and top and bottom plate will be called a clause filter. We can cascade clause filters to represent all the clauses in the 3-SAT formula, and the output slit of the m^{th} clause filter will contain short path classes only for those assignments (if any) which satisfy the formula.

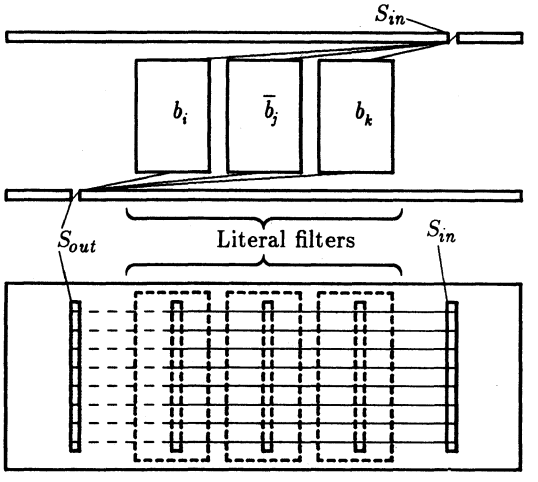

Figure 7: A clause filter.

The final step is to collect all these path classes into a single path class. This is done using a series of n inverted splitters. The effect is to form the disjunction of all the satisfying assignments. In the absence of any barriers in the preceding clause filters, there would be a single path class in the output slit and a single virtual source. Below this slit and aligned with the source, we place the target point q'. Let l be the approximate length of the shortest path from q to q' when the barriers are removed. We then ask if the shortest path from q to q' in an environment containing barriers has length close to l. It will if and only if there is some path through the environment which was not stretched by having to go around a barrier. Such a path encodes a satisfying assignment to the formula, and since we have encoded all possible assignments, the path has length close to l (see section 2.4 for a precise definition) if and only if the formula is satisfiable. Finally, by the results of section 2.5, the description of the environment has size polynomial in n and m and can be computed in polynomial time. □

Corollary 2.3.3 *Determining even the sequence of edges touched by the shortest path (under an L^p metric) is NP-hard.*

Proof Each path class is uniquely determined by the sequence of splitter edges it touches. Thus this sequence of edges encodes a satisfying assignment to the 3-SAT formula, if one exists.

Corollary 2.3.4 *For a polyhedral environment of size N, determining $O(\sqrt{N})$ bits of the length of the shortest path between two points in the environment is NP-hard.*

Proof. We first construct an environment that encodes a 3-SAT formula of length $\sqrt[4]{N}$ so that m and n are both less than $\sqrt[4]{N}$. Using the values computed in section 2.5, we notice that the value of ϵ defined in (12) leads to a gap between the upper bound on unstretched length and the lower bound on stretched length. This gap is at least $2^{-2nm-3n-3}$, so that $O(nm) = O(\sqrt{N})$ bits suffice to distinguish stretched and unstretched paths. □

2.4 The Virtual Source Approximation

Here we show that an approximate virtual source can be used to accurately model the path lengths at the input and output of a shortest path splitter or shuffler. We show that the error at the output of a shortest path splitter is 5ϵ greater than the error at its input. The proof generalizes to shufflers which have four plates rather than three and gives a bound of 7ϵ.

First we define a local coordinate system for each slit, fixed at one end of the slit (say the end closest to paths which encode 0). Let the t coordinate measure position along the slit. Thus t lies in the range $[0, l]$ where l is the length of the slit. Let u, and v measure respectively the horizontal and vertical position of a point in the slit, so that u and v both lie in the range $[0, \epsilon]$. If u increases in the upward direction, the position of the coordinate origin in the slit is completely determined when we add the constraint that the t-u-v system be right-handed.

Let $d^i(x, q)$ denote the distance of the shortest path in the i^{th} path class from a point $x = (t, u, v)$ in the slit to the actual source q. Let $\hat{d}(x, p_i)$ be the straight-line distance from x to the i^{th} virtual source p_i.

Lemma 2.4.1 *The following bound holds at the output of the n^{th} cascaded splitter or half-shuffler:*

$$\hat{d}(x, p_i) \leq d^i(x, q) \leq \hat{d}(x, p_i) + (5n + 2)\epsilon \qquad (3)$$

Furthermore, $\hat{d}(x, p_i)$ is independent of the u and v coordinates, i.e. we can write $\hat{d}(x, p_i) = \hat{d}(t, p_i)$. In this way we can think of the slit as being one-dimensional, and absorb the values of the u and v coordinates in the error term. The virtual source p_i is specified by two values, its t coordinate $t_i = i\delta t$, assuming sources are uniformly spaced by δt, and a distance h normal to the t axis, (h is the same for all sources in a given slit, so we drop the subscript i). Thus we have a simple expression for $\hat{d}(x, p_i)$:

$$\hat{d}(x, p_i) = ||(t_i - t, h, 0)||^p \qquad (4)$$

where $x = (t, u, v)$ as before. Our proof of the output hypothesis will be essentially the same for both splitters and half-shufflers, since we only need to consider one edge of the middle plate.

Base case:

If $n = 0$ have only the true source point q above the center of the first input slit. Let h be the height of the source above the slit. Then clearly $\hat{d}(x, p_i)$ from (4) is a lower bound on the distance to any point in the slit, where $p_i = q$ and t_i is half the length of the slit. On the other hand, $\hat{d}(x, q) + 2\epsilon$ is a valid upper bound because every point in the slit is within 2ϵ (under any L^p metric) of a point at the top of the slit whose distance is $\hat{d}(x, q)$ from the source.

Inductive step:

We assume the hypothesis holds at the output of the n^{th} splitter, and consider the path from input to output of the $(n+1)^{st}$. We first obtain a lower bound on the path length between any a point x in the input slit and a point x' in the output slit. For lower bounds, we consider the projection of paths in the x-y plane, since these lengths are less than or equal to the three-dimesional lengths.

For $\epsilon = 0$, let x'' be the point at which the path between x and x' touches the middle plate. Then the total length of the path from the source to x' is bounded below by

$$\hat{d}(x, p_i) + ||x'' - x||^p + ||x', x''||^p \qquad (5)$$

For each such path, we form a second path by reflecting the first two path segments about the middle slit, similar to figure 3. The mirror image path will have the same length as the original under any L^p metric if the middle slit is either parallel to the x or y axis, or at 45° to these axes. We can always build our environment so that this is the case. The length of the three segment path from x' to the mirror image p_i' of the virtual source p_i is bounded below by the straight line distance from x' to p_i' (this follows from the triangle inequality, which holds for any metric). Thus we have

$$\hat{d}(x', p_i') \geq ||(t' - t_i', h + l, 0)||^p \qquad (6)$$

where $x' = (t', u', v')$ is given in local slit coordinates.

We can also obtain an upper bound on the length of the shortest path between x and x'. To do this we build a path which consists of the horizontal straight line segments in the path for $\bar{e} = 0$, plus three vertical jumps of ϵ. This path moves vertically from the input slit to the top of the middle plate, horizontally to the to edge of the middle plate, vertically to the bottom edge of the middle plate, horizontally along the bottom surface of the middle plate, and vertically down to the output slit. Finally we need an upper bound which is valid throughout the bottom slit, which may involve traversing the slit in the u and v directions, an extra distance of at most 2ϵ, giving us a total of 5ϵ more than the lower bound for the distance between x and x'. Thus if the upper bound on path length at the input is $\hat{d}(x, p_i) + (5n + 2)\epsilon$, the upper bound at the output is $\hat{d}(x', p_i') + (5(n + 1) + 2)\epsilon$. □

2.5 Environment Size

To complete our construction, we must verify that the environment we have defined has a polynomial length description. In particular, we must find the constraints on ϵ for the virtual

source approximation to be valid, and ensure that it requires only polynomially many bits. We show furthermore that:

Lemma 2.5.1 *Every environment dimension can be described with $O(nm)$ bits.*

Proof. We first observe that the output slit of a splitter has twice the length of its input slit. We set the length of the top slit (arbitrarily) to be 1. Then after n splitters, we will have a slit of length 2^n with unit spacing between virtual sources. This is the maximum length of any structure in the environment. So we have

Remark 2.5.2 *All dimensions in the environment are $O(2^n)$.*

A shuffler's output slit has half the length of its input slit. Each clause filter consists of n shufflers in cascade, and there are m clause filters in series, so at the output of the last filter we have a slit of length $2^{n(1-m)}$ with virtual sources spaced by 2^{-nm}. All the slits in between have length and spacing in between these two extremes.

When a barrier blocks off half of a particular slit, every path that previously passed through the barrier is displaced horizontally by at least half the source spacing at that slit. For the L^1 metric we assume that the input and output slits of all stages are aligned with the x or y axis, then the new path has length

$$l_{stretched} \geq l + \delta_{min} \qquad \text{for } p = 1 \tag{7}$$

where l is the lower bound on the unstretched length of the path from source to target, and δ_{min} is the minimum source spacing. For all other L^p metrics, we align the input and output slits at 45° to the x and y axes. Recall that "mirror image" paths have the same length in either case. Then the length of the shortest stretched path is bounded below by

$$l_{stretched} \geq 2^{-\frac{1}{p}} \sqrt[p]{|l + \delta_{min}|^p + |l - \delta_{min}|^p} \qquad \text{for } 1 < p \leq \infty \tag{8}$$

where l is the lower bound, this time under the L^p metric, on the path length. For $p = \infty$, we take the limit of the above expression as $p \to \infty$. Now l is the sum of all the slit lengths plus the distance to source and target points, which we can adjust so that $l = 2^{3n}$. So long as $\delta_{min} \leq 1$, the following lower bound holds for all metrics:

$$l_{stretched} \geq l + \frac{\delta_{min}^2}{4l} \qquad \text{for } 1 \leq p \leq \infty \tag{9}$$

To obtain this bound, we raise the right-hand sides of equations (8) and (9) to the p^{th} power, and compare the $2i^{th}$ degree term from (8) with the sum of the i^{th} and $(p-i+1)^{th}$ terms from (9). Since our proof requires that we can decide whether a path has been stretched, we must have the difference between stretched and unstretched lengths greater than the error in our source approximation. Now the actual unstretched length $l_{unstretched}$ is subject to the following bound (for all metrics):

$$l \leq l_{unstretched} \leq l + (7nm + 10n + 2m + 4)\epsilon \tag{10}$$

since there are nm shufflers in cascade with $2n$ splitters each adding 7ϵ and 5ϵ error respectively, and 2ϵ error for the source, target and clause filter plates. To be able to detect a stretched path, we must have the lower bound on stretched length greater than the upper bound on unstretched length, i.e.

$$\frac{\delta_{min}^2}{4l} > (7nm + 10n + 2m + 4)\epsilon \tag{11}$$

and using the fact that $\delta_{min} = 2^{-nm}$ and $l = 2^{3n}$, the above inequality holds if we set:

$$\epsilon = \frac{2^{-2nm-3n-3}}{(7nm + 10n + 2m + 4)} \tag{12}$$

and then ϵ can be specified with $O(nm)$ bits. The entire environment fits in a cube of size $l = 2^{3n}$, and the smallest dimensions that need to be specified are of size approximately ϵ, thus the specification of any dimension in the environment requires $O(nm)$ bits. □

Corollary 2.5.3 *The entire environment can be described with $O(N^4)$ bits, where N is the length of the input SAT formula.*

Proof The environment consists of $3m$ shufflers, and $2n$ splitters. Each shuffler consists of $O(n)$ plates with a fixed number of edges and vertices. Each splitter has a fixed number of faces, edges and vertices. Thus there are $O(nm)$ edges, vertices and faces in the environment each of which can be specified with $O(nm)$ bits, and since both n and m are linear in the formula length N, our construction can be specified in space $O(N^4)$, and computed in polynomial time. □

3 Dynamic Motion Planning

3.1 Lower Bounds for the Asteroid Avoidance Problem

We can generalize the proof technique of the last section to motion planning with moving obstacles, where the robot has velocity limits. We have

Theorem 3.1.1 *The 2-d asteroid avoidance problem is NP-hard.*

Proof The proof follows from the results of the previous section if we can construct splitters and shufflers and specify their dimensions with a polynomial number of bits. A single construction can be adapted to implement both functions, and is shown in figures 8 and 9. We assume the velocity limit is 1. In this case, two points are in the same path class if they can be reached by a homotopically equivalent sequence of motions, i.e. p and q are in the same path class if we can continuously change the sequence of motions that lead to p into a sequence that leads to q, without colliding with obstacles. In our construction, path classes at a given time are approximately circular. Figure 8 shows four circular path classes which were points at some earlier time. Two moving obstacles in figure 8 effectively form two copies of the path classes, one moving up and the other moving down with velocity 1. Figure 9 shows a second obstacle B, which is moving very fast almost parallel to its lower edge, but nevertheless the normal component of this velocity is still 1. Thus the two copies of the path classes are pushed back together, but the

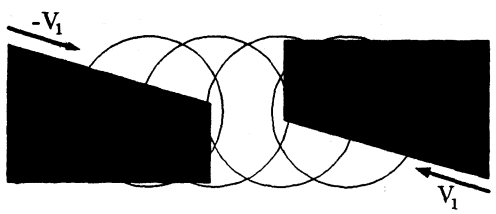

Figure 8: Path splitter in an asteroid environment.

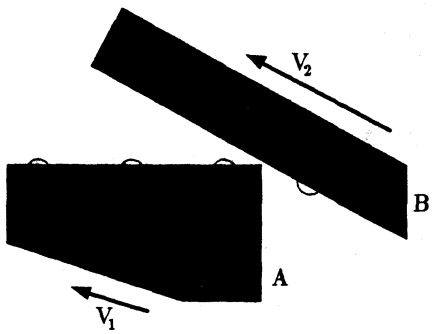

Figure 9: Path "reflection" for the asteroid problem. Path classes on object B move normal to B at the maximum velocity.

two obstacles B do not collide. Instead, with their high velocity, they move off to the left and right while leaving small slivers of the path classes intact. Depending on the direction of the second motion and the distance travelled during the first motion, the path classes may either be concatenated for a split, or their upper and lower halves interleaved for a shuffle. In the latter case, fast-moving vertical obstacles destroy the unused path classes, or may be used to select a particular literal.

Quantitatively, we suppose that each path class after the i^{th} shuffle is contained in a rectangle of height h_i and width w_i, and that it contains a circle of diameter h_i. Then if the angle between V_1 and the x-axis is θ_i, and the distance traveled in the first motion is l, we define $h_i' = g$ where g is the gap between A and B, and

$$w_i' = (w_i + \sqrt{lh_i})\cos 2\theta_i + h_i \sin 2\theta_i \qquad (13)$$

as the dimensions of an approximate bounding rectangle (aligned with B) at the end of the first motion. Then the path class at the completion of the second motion is contained in a rectangle of size $h_{i+1} = h_i$ and

$$w_{i+1} \leq w_i' + \sqrt{lg} \qquad (14)$$

Let n be the number of variables and m the number of clauses in a 3-SAT formula which we wish to encode. Then by choosing $\sin\theta_i \approx 2^{-i-1}$, $l = 1$, $h_i = g = 2^{-4mn}$, $w_1 = 2^{-2mn}$, and an initial spacing of 2^{-n} for the path classes, the above recurrence shows that the path classes remain distinct. Furthermore, all the dimensions and velocities of obstacle polygons are simple rational functions of these quantities. Thus we can specify a dynamic environment which encodes a 3-SAT formula of n variables and m clauses in $O(m^2n^2)$ space and polynomial time. □

4 Motion Planning with Uncertainty

In our proof we construct, for any non-deterministic exponential time bounded Turing machine M, an environment that simulates that machine. We assume *wlog* that M has a binary tape (of exponential size), which initially contains its input. Given a description of M and its input, and a constant c such that the running time of M is bounded by 2^{cn}, we construct a polynomial-size environment and start and goal regions and specify an uncertainty such that a successful motion plan exists if and only if the non-deterministic machine M has a path to an accepting state. At the i^{th} step, let $q(i)$ be the internal state of M, $h(i)$ its head position, and $T(i,j)$ the contents of the j^{th} tape square. We define the *local state* of M as the pair $\langle q(i), T(i,h(i))\rangle$.

At the start of a motion plan, the point p is somewhere in the start region S. When we execute the plan, at each time t there is a set of possible positions of p. We call this set the *instantaneous forward projection* of S and denote it $F_S(t)$, see [Er]. The instantaneous forward projection will consist of a number of connected components which we will call *blots*. The physical interpretation of this is that p at time t may lie anywhere inside any of the blots. We use the forward projection to represent the state of the Turing machine. The points in each blot are related by a homotopy of paths from the start region. Thus we are again making use of a path encoding scheme, and we will be generating exponentially many blots to encode an exponential tape.

In fact, using a proof very similar to those of the previous section, we can show that verifying a single step of a motion plan with uncertainty (with or without sliding) in 3 dimensions is hard. That is:

Theorem 4.0.2 *Determining whether a point p is in the forward projection $F_S(t)$ at some time t for a fixed commanded velocity is NP-hard.*

4.1 Blot Motion

The blot model allows a simple characterization of the time evolution of the forward projection. All blots are assumed to be contained in spheres of radius $r(t)$, satisfying the following condition:

$$r(t) = \epsilon_0 + \epsilon t \qquad (15)$$

so that the environment is initialized with all blots contained in spheres of radius ϵ_0. If a blot at time t is contained in a sphere of center $c(t)$, it should be fairly clear from (1) that if we command a motion v_i for time t_i, and the blot does not encounter obstacles, the center of the blot is simply displaced to $c(t) + v_i t_i$.

If the commanded motion moves the center of the blot into a wall, then the motion of the center of the blot can be broken into two parts: a straight line motion in the direction of commanded motion, and then motion along the wall with velocity equal to the projection of the commanded velocity

along the wall. In other words, the center of the blot moves compliantly as though there were no motion error.

It is easy to verify that blots satisfy the radius condition (15) for all motions except those where the blot is moved into a convex edge or corner. We will make use of this later to give us a splitting of blots, but generally these motions are to be avoided.

4.2 The Environment

Our environment can be broken into three distinct and physically separated polyhedral structures:

- Legal move filter. According to our model, it is possible to command any motion in any direction at each step. However, we would like the commanded motions to give us an orderly simulation of a Turing machine. We must therefore restrict the allowable motions to certain legal moves. The legal move filter enforces this by making it impossible to reliably reach the goal by *any* sequence of moves after an illegal move.
- Tape logic. When legal moves are executed, this structure performs the necessary updates on the tape itself, changing tape contents, head position and tape end marker fields.
- State logic. This structure performs updates on blots that represent the internal state of the Turing machine.

Initially, all of these structures contain some blots of forward projection. Now each legal move corresponds to a certain local state transition. However, the legal move filter does not examine tape contents or machine state, so at each step, the motion corresponding to every possible state transition is *legal*, even if the simulated machine is not in the state assumed by the transition. We say a legal move is *valid* if it does correspond to a Turing machine transition, given the current local state of the simulated machine. The tape and state logic structures ensure that if legal but *invalid* move is executed, then no later sequence of legal moves can reliably move the point to the goal. Thus the only possible way to reliably reach the goal is by executing a sequence of valid moves, thereby simulating Turing machine steps.

4.3 Legal Move Filter

The key to the simulation is to constrain *commanded* motions which may otherwise be arbitrary to a small set of motions in the x-y plane. Since the planner is free to command any motion it desires, we must build the environment in such a way that after an undesired motion, no subsequent sequence of motions can move the point to the goal. It is clear that we can constrain the motion of individual blots by placing them in a narrow channel (e.g. [Na]). Unfortunately, since we have exponentially many blots we cannot use this technique. Consider now figure 10. Here there are two blots in two distinct boxes, and we must command a sequence of motions that is guaranteed to move both blots into their respective goal regions. It is fairly clear that a sequence of purely horizontal motions will succeed, as long as the last motion terminates inside the goal, and there are not too many motions (because of the growth due to uncertainty). Suppose on the other hand, that we execute a single motion with a

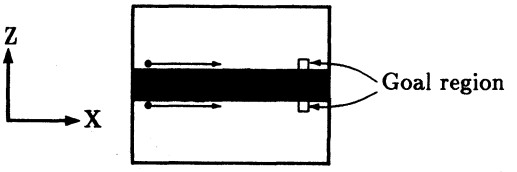

Figure 10: A filter for motion in the x-y plane.

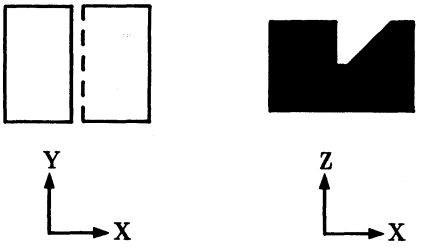

Figure 11: A filter for horizontal motion in the left half-plane.

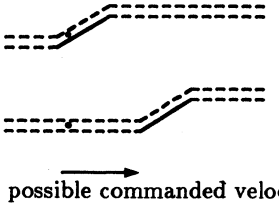

Figure 12: A one-way gate.

fixed vertical displacement of h, say upward. The bottom blot will move away from the wall by h, while the other will slide against its wall. In order to move the displaced blot to the goal, we must eventually make a motion with a downward component, but this will move the other blot away from its wall etc. Thus once a motion with a vertical displacement is executed, no sequence of motions can move both blots into the goal region. This environment functions as a filter for commanded motions, and allows only horizontal ones.

Quantitatively, if the height of the goal region is δ, and if the commanded motion causes a net vertical displacement of the center of a free blot at any time $t < t_f$ of greater than $2(\delta + \epsilon t_f)$, then from the laws of blot motion, the sum of the distances of the blot centers from the surfaces must be at least $2(\delta + \epsilon t_f)$, and can never be made less than this. It follows that one of the two blots must be entirely outside the goal at time t_f.

Once we have constrained the commanded motions to the x-y plane (or to within a region of height $2(\delta + \epsilon t_f)$), we can add a variety of other constraints. Figure 11 shows a structure which constrains the commanded motion directions to a semicircle. Commanding motion into a vertical wall (shown solid) is permissible, and causes sliding in the horizontal plane, but commanding motion into a sloped wall (dashed) causes the blot to be displaced vertically. If the goal region is at the same height as the start region, the blot in this environment can never reach it once it has been displaced upward. Figure 12 shows a structure which contains two blots, and implements a one-way gate.

The legal move filter is shown in figure 13. Notice that all motions are in the x-y plane. The channels at move 3

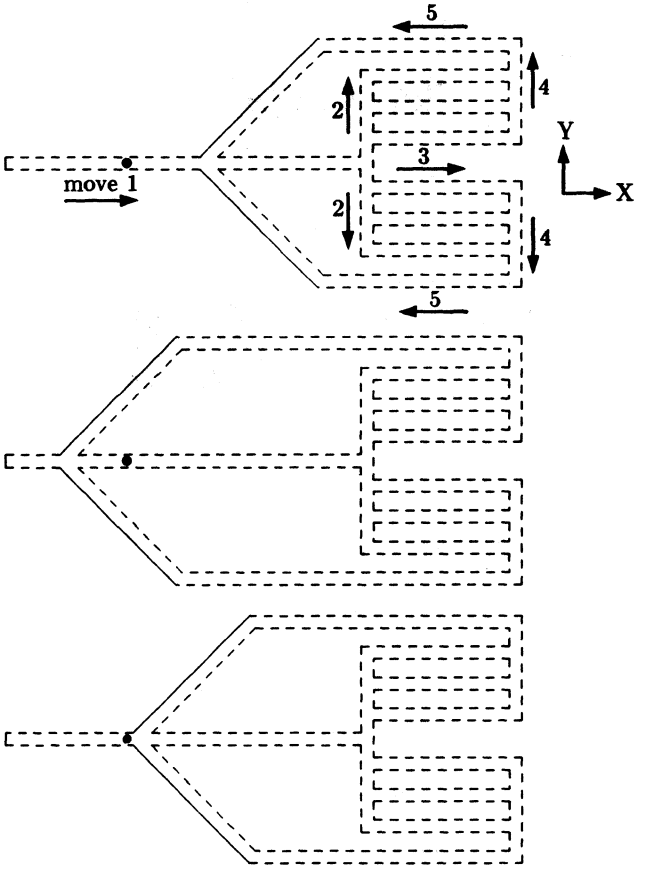

Figure 13: The legal move filter, consisting of three boxes.

all have one-way gates of the type shown in figure 12, which are not shown in figure 13 for simplicity. Each distinct y-level at move 3 corresponds to a particular Turing machine transition, and is indexed by the local state of M. Observe that these transitions lead to overall displacement of the tape by one square either up or down, which corresponds to the correct head motion for that transition.

Notice that none of the structures in the legal move filter have an adjacent pair of vertical walls, so that blots cannot be split in this environment. The three blots move in unison except at move 5. Three structures are necessary to ensure that blots are not separated at move 5, and that only horizontal motion to the left is possible during move 5. Notice that after a cycle of moves 1 through 5, all blots terminate in their start positions. For moves 1, 2, and 4, commanded motions may in fact be in the forward or backward direction, and this will not affect the simulation. There are one-way gates at move 3 to ensure that blots do not move in the wrong direction through tape or state logic.

We claim that the total cumulative error during a move cycle, i.e. the error between the displacement of a free blot and the distance between tape squares (take this to be 1), is a small constant times the channel width. If M runs for 2^{cn} steps (n is the input length), then we need a linear number of bits to specify ϵ and channel width small enough that the cumulative error is a small fraction of the distance between tape squares. All environment dimensions are linear in n.

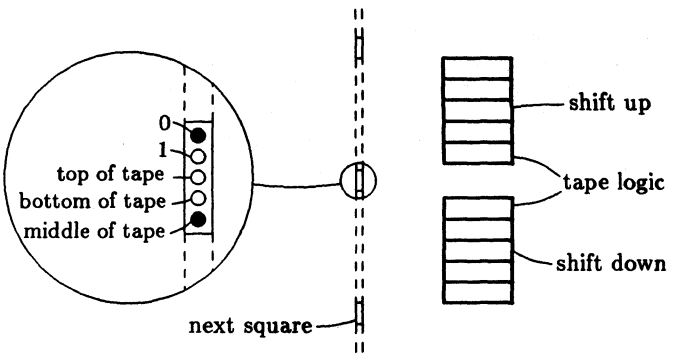

Figure 14: Tape encoding.

4.4 Tape and State Logic Structures

In order that a legal move be valid, the $\langle q(i), T(i, h(i))\rangle$ pair assumed by the move must correspond to the actual local state encoded when the move is executed. For a nondeterministic machine there may be several valid moves for a given local state. The tape and state logic structures ensure that only commanded motions that simulate valid transitions can possibly lead to the goal.

Our machine has a binary tape, and the encoding of a single square includes two rectangular regions, one to encode 0, the other 1. Exactly one of the sites must contain a blot of forward projection. Also, we have a tape end marker field with three sites, exactly one of which will contain a blot. These sites designate the square as the top, bottom or as an intermediate square. An example of an encoded tape is given in figure 14. Notice that the distance between tape squares is much larger than the height of each square.

Figure 15 shows a slice through tape and state structures at the j^{th} level. There will be a pair of such structures for each state transition of M. Notice that there is tape logic for only one square of the tape, namely the square currently under the head. An important difference between tape and state structures is that while the tape blots are free to move up or down during the tape shift phase of a legal motion (move 4), state blots are trapped in channels and funneled back to their original y position, as shown in figure 16.

If the legal move corresponding to this state transition is executed but the tape contents are not $T(i,(h(i))$, then some tape blot will run into a sloped wall and be displaced vertically. Otherwise, it will slide against a wall into the correct position for the value to be written on the tape. Similarly if the internal state before the move is not $q(i)$, the state transition structure will cause a blot to be displaced. Thus the legal move corresponding to the transition from $\langle q(i), T(i, h(i))\rangle$ will be valid if and only if the (simulated) tape contents really are $T(i, h(i))$ and the internal state is $q(i)$. Since validity of tape and state can be verified independently, tape and state structures can be physically separated.

Each level implements a state transition similar to the one described above, with the exception of transitions that require shifting beyond the limits of the tape. Such a transition is shown in figure 17, and denote this state transition by Q_{ij} . Here we notice that the square below the head is completely blank, but it must be correctly initialized during this move. Since there are only 2 blots entering the tape structure but

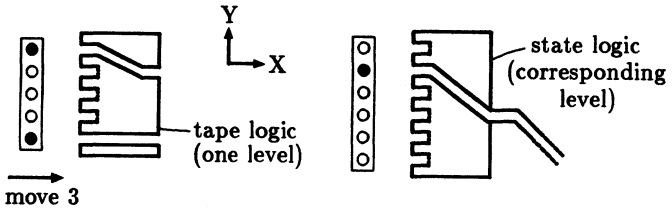

Figure 15: Tape and state logic (one level only).

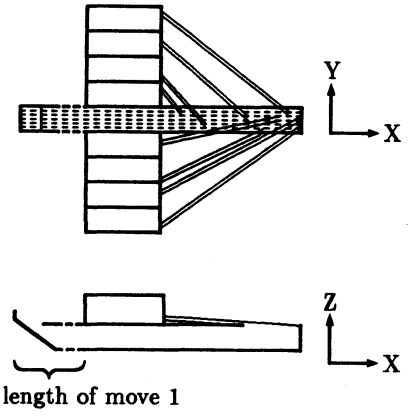

Figure 16: State logic (global view).

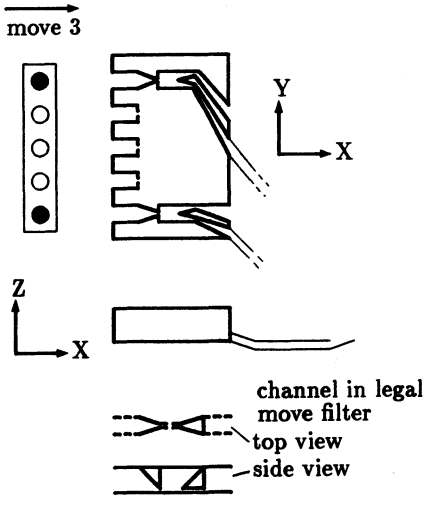

Figure 17: tape logic for shifting beyond the end of the tape

we need 4 to exit, we must split some of the entering blots, as shown in the figure. Special conduits carry the blots to the location of the new tape square, since this is at some distance from the tape logic. In order for this splitting to occur, we need tighter control that normal over the direction of the commanded velocity for this move. The structure shown in figure 17b is added at move 3 in one of the legal move filter structures at the y-level corresponding to Q_{ij}. It ensures that some part of the forward projection must pass over both sides of the splitter in figure 17.

4.5 Initialization and Termination

We have seen that tape and state logic structures allow only valid moves, and that any sequence of motions which reliably moves p to the goal must simulate Turing machine steps. To complete our simulation we must show that it can be correctly initialized and terminated. Initialization involves specification of the start region S, while termination involves specification of the goal region G.

Firstly, the start region must correctly describe the initial internal state of the machine. This requires only a single blot (of start region) in the appropriate channel of the state logic structure. The start region must also correctly describe the initial state of the tape. This is straightforward as the tape initially needs only a linear number of blots. This is because the tape need only represent the input data to the machine M, and as explained above, if we shift beyond the tape limits, the neighboring squares are correctly setup during move (3).

The legal move generator has its blots in goal regions only at the end of move 3. The goal region for the tape structure is simply a rectangular box large enough to contain all tape blots at the end of move 3. Thus all tape blots will be in the goal region after move 3 of any sequence of valid moves. The goal region for the state logic on the other hand, is a region at the exit from the machine's halt state Q_f. At this time the point p is guaranteed to be in the goal region, and so the sequence of valid moves constitutes a succesful motion plan. Such a plan exists if and only if the non-deterministic Turing machine M halts on (accepts) that input. Thus we have

Theorem 4.5.1 *Compliant Motion Planning with Uncertainty is Non-Deterministic Exponential Time Hard*

Proof We have described a polyhedral environment and start and goal regions such that a guaranteed motion plan exists if and only if M has a path to an accepting state. Since the amount of logic for each tape or state transition is constant, and since there is tape logic under only one square of the tape, the number of objects in the environment is polynomial in the length of the description of M. By the results of the previous sections, we need a polynomial number of bits to describe the structures and start and goal regions in the environment. Finally, the description of these structures can be computed in polynomial time. □

5 Conclusions

In this paper we used path encoding to give new lower bounds for three fundamental robot motion planning problems. We gave the first non-trivial lower bounds for 3-dimensional shortest path under any L^p metric. We showed that finding the shortest path is NP-hard, and that a polyhedral environment may contain exponentially many shortest path classes. The best known upper bounds require more than polynomial space, so that the exact complexity of the problem remains open. The difficulty in finding good bounds seems to stem from the fact that the problem has both a combinatorial (edge sequence touched) and an algebraic character (position of contact points on edges). We made use of the combinatorial aspect only in our NP-hardness proof.

However, knowing the edge sequence is not sufficient to determine the path, because the position of contact points on edges does not seem to be describable as a polynomial-size algebraic number, so there is no obvious NP or Σ_2 algorithm for

the problem. The contact points are defined by high degree polynomials, and Bajaj [Ba] has shown these polynomials are irreducible in some cases.

Notice that our proof requires some large rational numbers to describe the environment, and no longer succeeds if integers are coded in unary. Thus we have demonstrated NP-hardness but not strong NP-hardness. This is not surprising in the light of Papadimitriou's [Pa] approximate algorithm for the problem, which takes time polynomial in both the environment size and the length of a unary approximation error.

We showed that 2-dimensional dynamic motion planning with bounded velocity magnitude is NP-hard even with polygonal (in fact convex) obstacles moving with constant velocity. This result should readily generalize to the case where the velocity is bounded by any convex polygon, rather than a circle.

We also gave a non-deterministic exponential time hardness proof for the motion planning with uncertainty problem. Here control uncertainty was a fundamental limitation to our representation of state using path encoding. It seems plausible that the proof could be extended to exponential space hardness by periodically squeezing all of the state blots, with a "refresh" of the tape.

References

[Ba] Bajaj C., "The Algebraic Complexity of Shortest Paths in Polyhedral Spaces", Purdue University, Computer Science tech. rept. CSD-TR-523, (June 1985).

[BKR] Ben-Or M., Kozen D., and Reif J., "The Complexity of Elementary Algebra and Geometry", J. Comp. and Sys. Sciences, Vol. 32, (1986), pp. 251-264.

[Ca] Canny J. "A New Algebraic Method for Robot Motion Planning and Real Geometry", Proc. 28th IEEE Symp. FOCS, Los Angeles (Oct 1987).

[Co] Collins G.E. "Quantifier Elimination for Real Closed Fields by Cylindrical Algebraic Decomposition" Lecture Notes in Computer Science, No. 33, Springer-Verlag, New York, (1975), pp. 135-183.

[Er] Erdmann M. "On Motion Planning with Uncertainty", MIT AI Lab. rept. TR-810, (1984).

[HSS] Hopcroft J., Schwartz J., Sharir M., "On the Complexity of Motion Planning for Independent Objects: PSPACE-Hardness of the 'Warehouseman's Problem' ", Int. Jour. Robotics Research, vol 3, no 4, Winter (1984), pp. 76-88.

[In] Inoue H., "Force Feedback in Precise Assembly Tasks", MIT AI Lab memo 308, (August 1974).

[KY] Kozen D., and Yap C. "Algebraic Cell Decomposition in NC", Proc IEEE symp. FOCS, (1985), pp. 515-521.

[Lo] Lozano-Pérez T., "Spatial Planning: A Configuration Space Approach," IEEE Trans. Computers, C-32, No. 2 (Feb 1983) pp. 108-120.

[LMT] Lozano-Pérez T., Mason M., and Taylor R., "Automatic Synthesis of Fine Motion Strategies for Robots", Int. Jour. Robotics Research, vol 3, no 1, (Spring 1984), pp. 3-24.

[LW] Lozano-Pérez T., and Wesley M., "An algorithm for Planning Collision-Free Paths Among Polyhedral Obstacles", Comm. ACM, vol 22, no 10, (Oct 1979), pp. 560-570.

[Ma] Mason M., "Compliance and Force Control for Computer Controlled Manipulators", IEEE Trans. SMC, vol 11, no 6, (June 1981), pp. 418-432.

[MP] Mitchell J. S. B. and Papadimitriou C. H., "The Weighted Region Problem", Proc. 3rd ACM Symp. on Computational Geometry, Waterloo, Canada (June 1987), pp. 30-38.

[Mo] Mount D. M., "On finding shortest paths on convex polyhedra", Tech. Rept., Computer Science Department, University of Maryland, (1984).

[Na] Natarajan B. K., "On Moving and Orienting Objects", Cornell University, TR86-775, (1986).

[Pa] Papadimitriou C., "An Algorithm for Shortest-Path Motion in Three Dimensions" Inf. Proc. Letters, vol 20, (1985), pp. 259-263.

[Re] Reif J., "Complexity of the Mover's Problem and Generalizations," Proc. 20th IEEE Symp. FOCS, (1979). Also in "Planning, Geometry and Complexity of Robot Motion", ed. by J. Schwartz, M. Sharir, and J. Hopcroft, Ablex publishing corp. New Jersey, (1987), Ch. 11, pp. 267-281.

[RSh] Reif J., and Sharir M., "Motion Planning in the Presence of Moving Obstacles", Proc. 25th IEEE symp. FOCS, (1985), pp. 144-154.

[RSt] Reif J., and Storer J., "Shortest Paths in Euclidean Space with Polyhedral Obstacles", Tech. Rep. CS-85-121, Comp. Sci. Dept., Brandeis University, (April 1985).

[SSh] Schwartz J. and Sharir M., "On the 'Piano Movers' Problem, II. General Techniques for Computing Topological Properties of Real Algebraic Manifolds," in "Planning, Geometry and Complexity of Robot Motion", ed. by J. Schwartz, M. Sharir, and J. Hopcroft, Ablex publishing corp. New Jersey, (1987), Ch. 5, pp. 154-186.

[SB] Sharir M., and Baltsam A., "On Shortest Paths amid Convex Polyhedra", Proc. ACM Computational Geometry Conf., Yorketown Heights, 1986.

[SSc] Sharir M., and Schorr A., "On Shortest Paths in Polyhedral Spaces", Proc. 16th ACM STOC, (1984), pp. 144-153.